Research Article | Vol. 26, No. 4 | 19 Feb 2018 | OPTICS EXPRESS 4401
Optics EXPRESS

Radially polarized passively mode-locked thin-disk laser oscillator emitting sub-picosecond pulses with an average output power exceeding the 100 W level

FRIEDER BEIROW,* MICHAEL ECKERLE, BENJAMIN DANNECKER, TOM DIETRICH, MARWAN ABDOU AHMED, AND THOMAS GRAF

Institut für Strahlwerkzeuge (IFSW), Pfaffenwaldring 4, 70569 Stuttgart, Germany
**frieder.beirow@ifsw.uni-stuttgart.de*

Abstract: We report on a high-power passively mode-locked radially polarized Yb:YAG thin-disk oscillator providing 125 W of average output power. To the best of our knowledge, this is the highest average power ever reported from a mode-locked radially polarized oscillator without subsequent amplification stages. Mode-locking was achieved by implementing a SESAM as the cavity end mirror and the radial polarization of the LG^*_{01} mode was obtained by means of a circular Grating Waveguide Output Coupler. The repetition rate was 78 MHz. A pulse duration of 0.97 ps and a spectral bandwidth of 1.4 nm (FWHM) were measured at the maximum output power. This corresponds to a pulse energy of 1.6 µJ and a pulse peak power of 1.45 MW. A high degree of radial polarization of 97.3 ± 1% and an M^2-value of 2.16 which is close to the theoretical value for the LG^*_{01} doughnut mode were measured.

OCIS codes: (140.3460) Lasers; (140.3480) Lasers, diode-pumped; (140.3580) Lasers, solid-state; (140.3300) Laser beam shaping; (140.7090) Ultrafast lasers; (230.1950) Diffraction gratings.

References and links

1. Q. Zhan, "Cylindrical vector beams: From mathematical concepts to applications," Adv. Opt. Photonics **1**(1), 1–57 (2009).
2. V. G. Niziev and A. V. Nesterov, "Influence of beam polarization on laser cutting efficiency," J. Phys. D **32**(13), 1455–1461 (1999).
3. R. Weber, A. Michalowski, M. Abdou Ahmed, V. Onuseit, V. Rominger, M. Kraus, and T. Graf, "Effects of Radial and Tangential Polarization in Laser Material Processing," Phys. Procedia **12**, 21–30 (2011).
4. T. Häcker, "Adapted polarization for sheet metal cutting," in *AKL International Laser Technology Congress* (2016).
5. M. Kraus, M. A. Ahmed, A. Michalowski, A. Voss, R. Weber, and T. Graf, "Microdrilling in steel using ultrashort pulsed laser beams with radial and azimuthal polarization," Opt. Express **18**(21), 22305–22313 (2010).
6. C. Hnatovsky, V. G. Shvedov, and W. Krolikowski, "The role of light-induced nanostructures in femtosecond laser micromachining with vector and scalar pulses," Opt. Express **21**(10), 12651–12656 (2013).
7. E. Skoulas, A. Manousaki, C. Fotakis, and E. Stratakis, "Biomimetic surface structuring using cylindrical vector femtosecond laser beams," Sci. Rep. **7**(45114), 45114 (2017).
8. S. Quabis, R. Dorn, and G. Leuchs, "Generation of a radially polarized doughnut mode of high quality," Appl. Phys. B **81**(5), 597–600 (2005).
9. G. Machavariani, Y. Lumer, I. Moshe, A. Meir, and S. Jackel, "Efficient extracavity generation of radially and azimuthally polarized beams," Opt. Lett. **32**(11), 1468–1470 (2007).
10. I. Moshe, S. Jackel, and A. Meir, "Production of radially or azimuthally polarized beams in solid-state lasers and the elimination of thermally induced birefringence effects," Opt. Lett. **28**(10), 807–809 (2003).
11. G. Machavariani, Y. Lumer, I. Moshe, A. Meir, S. Jackel, and N. Davidson, "Birefringence-induced bifocusing for selection of radially or azimuthally polarized laser modes," Appl. Opt. **46**(16), 3304–3310 (2007).
12. A. Ito, Y. Kozawa, and S. Sato, "Selective oscillation of radially and azimuthally polarized laser beam induced by thermal birefringence and lensing," J. Opt. Soc. Am. B **26**(4), 708–712 (2009).
13. M. P. Thirugnanasambandam, Y. Senatsky, and K. Ueda, "Generation of radially and azimuthally polarized beams in Yb:YAG laser with intra-cavity lens and birefringent crystal," Opt. Express **19**(3), 1905–1914 (2011).
14. S. Vyas, Y. Kozawa, and S. Sato, "Generation of radially polarized Bessel-Gaussian beams from c-cut Nd:YVO_4 laser," Opt. Lett. **39**(4), 1101–1104 (2014).

#318091 https://doi.org/10.1364/OE.26.004401
Journal © 2018 Received 20 Dec 2017; revised 2 Feb 2018; accepted 5 Feb 2018; published 9 Feb 2018

Optics EXPRESS

15. M. Endo, "Azimuthally polarized 1 kW CO2 laser with a triple-axicon retroreflector optical resonator," Opt. Lett. **33**(15), 1771–1773 (2008).
16. Y. Kozawa and S. Sato, "Generation of a radially polarized laser beam by use of a conical Brewster prism," Opt. Lett. **30**(22), 3063–3065 (2005).
17. T. Kämpfe, S. Tonchev, A. V. Tishchenko, D. Gergov, and O. Parriaux, "Azimuthally polarized laser mode generation by multilayer mirror with wideband grating-induced TM leakage in the TE stopband," Opt. Express **20**(5), 5392–5401 (2012).
18. M. A. Ahmed, A. Voss, M. M. Vogel, and T. Graf, "Multilayer polarizing grating mirror used for the generation of radial polarization in Yb:YAG thin-disk lasers," Opt. Lett. **32**(22), 3272–3274 (2007).
19. D. Lin, J. M. O. Daniel, M. Gecevičius, M. Beresna, P. G. Kazansky, and W. A. Clarkson, "Cladding-pumped ytterbium-doped fiber laser with radially polarized output," Opt. Lett. **39**(18), 5359–5361 (2014).
20. M. A. Ahmed, J. Schulz, A. Voss, O. Parriaux, J.-C. Pommier, and T. Graf, "Radially polarized 3 kW beam from a CO2 laser with an intracavity resonant grating mirror," Opt. Lett. **32**(13), 1824–1826 (2007).
21. C. J. Saraceno, F. Emaury, O. H. Heckl, C. R. E. Baer, M. Hoffmann, C. Schriber, M. Golling, T. Südmeyer, and U. Keller, "275 W average output power from a femtosecond thin disk oscillator operated in a vacuum environment," Opt. Express **20**(21), 23535–23541 (2012).
22. C. J. Saraceno, F. Emaury, C. Schriber, M. Hoffmann, M. Golling, T. Südmeyer, and U. Keller, "Ultrafast thin-disk laser with 80 µJ pulse energy and 242 W of average power," Opt. Lett. **39**(1), 9–12 (2014).
23. D. Bauer, I. Zawischa, D. H. Sutter, A. Killi, and T. Dekorsy, "Mode-locked Yb:YAG thin-disk oscillator with 41 µJ pulse energy at 145 W average infrared power and high power frequency conversion," Opt. Express **20**(9), 9698–9704 (2012).
24. J. Brons, V. Pervak, E. Fedulova, D. Bauer, D. Sutter, V. Kalashnikov, A. Apolonskiy, O. Pronin, and F. Krausz, "Energy scaling of Kerr-lens mode-locked thin-disk oscillators," Opt. Lett. **39**(22), 6442–6445 (2014).
25. A. Loescher, J.-P. Negel, T. Graf, and M. Abdou Ahmed, "Radially polarized emission with 635 W of average power and 2.1 mJ of pulse energy generated by an ultrafast thin-disk multipass amplifier," Opt. Lett. **40**(24), 5758–5761 (2015).
26. A. Loescher, J.-P. Negel, T. Graf, W. Pallmann, B. Resan, I. Martial, J. Didierjean, F. Lesparre, J.-T. Gomes, X. Delen, F. P. Druon, F. Balembois, P. Georges, and M. Abdou Ahmed, "A 265W and 782 fs amplified radially polarized beam emitted by a thin-disk multipass amplifier," in *Advanced Solid State Lasers*, OSA Technical Digest (online) (Optical Society of America, 2015), paper ATh3A.3.
27. M. Eckerle, T. Dietrich, F. Schaal, C. Pruss, W. Osten, M. A. Ahmed, and T. Graf, "Novel thin-disk oscillator concept for the generation of radially polarized femtosecond laser pulses," Opt. Lett. **41**(7), 1680–1683 (2016).
28. J.-P. Negel, A. Voss, M. Abdou Ahmed, D. Bauer, D. Sutter, A. Killi, and T. Graf, "1.1 kW average output power from a thin-disk multipass amplifier for ultrashort laser pulses," Opt. Lett. **38**(24), 5442–5445 (2013).
29. F. Lesparre, J. T. Gomes, X. Délen, I. Martial, J. Didierjean, W. Pallmann, B. Resan, M. Eckerle, T. Graf, M. Abdou Ahmed, F. Druon, F. Balembois, and P. Georges, "High-power Yb:YAG single-crystal fiber amplifiers for femtosecond lasers in cylindrical polarization," Opt. Lett. **40**(11), 2517–2520 (2015).
30. C. Kerse, H. Kalaycıoğlu, P. Elahi, B. Çetin, D. K. Kesim, Ö. Akçaalan, S. Yavaş, M. D. Aşık, B. Öktem, H. Hoogland, R. Holzwarth, and F. O. Ilday, "Ablation-cooled material removal with ultrafast bursts of pulses," Nature **537**(7618), 84–88 (2016).
31. A. Ancona, F. Röser, K. Rademaker, J. Limpert, S. Nolte, and A. Tünnermann, "High speed laser drilling of metals using a high repetition rate, high average power ultrafast fiber CPA system," Opt. Express **16**(12), 8958–8968 (2008).
32. B. Weichelt, A. Voss, M. Abdou Ahmed, and T. Graf, "Enhanced performance of thin-disk lasers by pumping into the zero-phonon line," Opt. Lett. **37**(15), 3045–3047 (2012).
33. C. J. Saraceno, F. Emaury, C. Schriber, A. Diebold, M. Hoffmann, M. Golling, T. Sudmeyer, and U. Keller, "Toward Millijoule-Level High-Power Ultrafast Thin-Disk Oscillators," IEEE J. Sel. Top. Quantum Electron. **21**(1), 106–123 (2015).
34. T. Dietrich, S. Piehler, C. Röcker, M. Rumpel, M. Abdou Ahmed, and T. Graf, "Passive compensation of the misalignment instability caused by air convection in thin-disk lasers," Opt. Lett. **42**(17), 3263–3266 (2017).
35. M. Haiml, R. Grange, and U. Keller, "Optical characterization of semiconductor saturable absorbers," Appl. Phys. B **79**(3), 331–339 (2004).
36. T. Liebig, M. Abdou Ahmed, A. Voss, and T. Graf, "Novel multi-sensor polarimeter for the characterization of inhomogenously polarized laser beams," in *SPIE LASE Photonics West* (2010).

1. Introduction

Radially and azimuthally polarized laser beams have attracted a great interest within different fields of scientific applications such as optical trapping, imaging or plasmon excitation [1]. In laser material processing, the advantages of radially and azimuthally polarized beams over circularly or linearly polarized beams have been theoretically outlined for cutting with CO_2 lasers in [2]. An increase of the cutting speed of up to a factor of 2 for radially polarized beams in comparison to circularly or linearly polarized beams was predicted. Experimentally an increase of the cutting speed of 37.5% by using a radially polarized rather than a circularly

Optics EXPRESS

polarized CO_2 laser was demonstrated [3]. Using a wavelength of 1.03 µm an increase of the cutting speed of 42.9% for a radially polarized beam in comparison to an unpolarized beam was shown [4]. For deep-penetration welding with low speeds at a wavelength of 1 µm a significant reduction of spattering could be realized using azimuthally polarized beams. The aforementioned results were obtained using continuous wave beams. In [5] it was shown that the use of azimuthally polarized picosecond laser pulses is beneficial for the production of holes with high aspect ratios in steel. Moreover, a better quality of micro holes in fused silica and silicon was obtained using femtosecond laser beams with radial polarization [6]. Recently, biomimetic structures giving rise to e.g. the water repellent lotus-leaf effect on metallic surfaces were fabricated with radially and azimuthally polarized femtosecond laser pulses [7].

There are two approaches to generate radially and azimuthally polarized beams. In the extra-cavity approach a linearly polarized fundamental mode is converted to a radially polarized LG^*_{01} mode using a transmissive or reflective optical component. This component locally rotates the polarization of the incoming beam such that it corresponds to the desired polarization state. One example of such a polarization converter consists of e.g. eight half-wave plate segments with different orientations of the fast axis [3, 8, 9]. The conversion efficiency of such a converter is however limited to approx. 90% and further beam clean-up is required to obtain good beam quality. Irrespective of the beam quality, a high degree of radial polarization of up to 98% was shown [9]. The intra-cavity approach generates the LG^*_{01} mode directly inside the laser cavity by a proper resonator design. For solid-state bulk lasers birefringence effects can be used to select a radially or azimuthally polarized LG^*_{01} mode [10–14]. Another possibility is to introduce an optical element into the laser cavity that introduces losses to the unwanted polarization states as for instance a triple axicon retroreflector [15] or a conical Brewster prism [16]. Especially at high powers sub-wavelength gratings proved to be very suitable devices to generate radially and azimuthally polarized LG^*_{01} modes inside of solid-state bulk [17], thin-disk [18], fiber [19] or CO_2 laser cavities [20].

In fundamental Gaussian transverse mode operation an average output power of 275 W [21] and a pulse energy of 80 µJ [22] was demonstrated with a SESAM mode-locked thin-disk oscillator operated in low-pressure atmosphere enclosure. The highest average output power obtained from a SESAM mode-locked thin-disk oscillator operated in ambient atmospheric air was 145 W [23]. An average output power of 270 W was demonstrated with a Kerr-Lens mode-locked thin-disk oscillator operated in ambient atmospheric air [24]. The highest average output power in radial polarization achieved from ultrafast lasers so far was achieved by converting a linearly polarized Gaussian seed beam into a radially polarized LG^*_{01} beam by means of an extra-cavity segmented half-wave plate converter and subsequent amplification by a thin-disk multipass amplifier. An average output power of 635 W with a pulse duration of around 8 ps [25] and an average output power of 265 W with a pulse duration of 782 fs [26] were demonstrated with this approach. To inject a radially polarized seed beam with sufficient average power to efficiently operate the thin-disk multipass amplifier either a commercial laser system (TRUMPF TruMicro 5050 in [25]) or a complex customized setup consisting of a multi-stage single-crystal fiber (SCF) pre-amplifier [26] was used. The segmented wave plate used to convert the polarization further introduces a power loss of ≥10% and causes diffraction at the edges of the individual segments, which requires a beam clean-up to ensure a high beam quality behind the polarization converter. These issues can be avoided by generating the radially polarized beam directly inside the laser cavity. Recently, the first SESAM mode-locked radially polarized Yb:YAG thin-disk oscillator providing 13.3 W of average output power with sub-picosecond pulses was demonstrated [27]. To be suitable as a seed for a multipass thin-disk laser amplifier, such a laser should however provide an average power of at least in the order of 100 W [28].

Optics EXPRESS

In the present paper we therefore report on a laser oscillator with improved power capability, which resulted in a record average output power of 125 W at a pulse repetition rate of 78 MHz. Compared to the previous report, this corresponds to an increase of the average output power by almost one order of magnitude and also outperforms the average powers of previously reported and more complex setups with the SCF amplifiers [29]. Hence, the oscillator presented in the following is a very promising seed source especially for thin-disk multipass amplifiers that should reach kW-level average output powers without complex and expensive pre-amplification stages.

In terms of pulse energy, amplifier based systems such as presented in [29] are still superior. But for the application of the so called ablation cooling regime which at the lower end begins at repetition rates of somewhere between 27 MHz and 108 MHz for copper [30] moderate pulse energies of a few µJ are sufficient. In this regime the authors of [30] observed an increase of the ablation efficiency by one order of magnitude as compared to the traditional ablation regime [31]. Consequently the presented oscillator might also contribute to increase the productivity in the field of material processing.

2. Experimental setup

An Yb:YAG thin-disk with a thickness of 215µm and a doping concentration of 7 at. % was used for the experiments. It was mounted on a diamond heat sink in order to ensure an optimum heat extraction from the pumped region. The disk was integrated into a standard pumping module allowing for 24 passes of the pump beam through the disk. The pump spot on the disk was set to a diameter of 3.6 mm. A laser diode with a wavelength of 969 nm was used to pump the crystal into the zero phonon line [32], which leads to a significant reduction of the thermal load on the disk compared to the pumping at 941 nm as applied in [27]. As a further improvement the oscillator was housed to shield it from air turbulences which destabilize the transversal mode as was observed with the setup reported in [27]. The cavity was designed such that the ratio between the diameter of the LG^*_{01} mode on the disk and the pump spot diameter corresponded to about 75%.

The set-up of the laser oscillator is sketched in Fig. 1(a) together with the radius of the oscillating laser mode at the positions along the propagation within the cavity in Fig. 1(b). In order to generate a radially polarized mode inside the cavity, a circular Grating Waveguide Output Coupler (GWOC) similar to the one used in [27] but with slightly different parameters, i.e. a grating period, depth and duty-Cycle of 900 nm, 24nm, and 50% respectively, was implemented as the output coupler. The spectral reflectivity measured with a radially and an azimuthally polarized probe beam is shown in Fig. 2(a). This GWOC exhibited a reflectivity of 95.2% for the radially polarized mode and a lower reflectivity of only 69.8% for the azimuthally polarized mode. This discrimination was sufficient to suppress the oscillation of azimuthally polarized radiation. The spectral reflectivity measured with a radially and an azimuthally polarized probe beam is shown in Fig. 2(a). A transmission of the GWOC of 2.7% for a radially polarized beam was measured indicating a power loss of 43.8% of the out-coupled power into the ± 1st diffraction order. Figure 2(b) illustrates this loss mechanism schematically. Minimizing the diffraction losses of the GWOCs is part of our ongoing work and will potentially lead to even higher obtainable average output powers. Soliton mode-locking was achieved by implementing a Semiconductor Saturable Absorber Mirror (SESAM) as the cavity end mirror. The parameters of this SESAM were specified by the supplier (Batop GmbH) as follows: modulation depth ΔR of 0.57%, saturation fluence F_{sat} of 26.65 µJ/cm^2, recovery time of 1 ps and non-saturable losses ΔR_{ns} of 0.06%. For a given intra-cavity pulse energy there is a tradeoff between the adaptation of the radius of the oscillating mode on the SESAM to meet the saturation fluence of this element and the fact that a larger beam on the SESAM leads to a stronger influence of thermal lensing on the resonator stability. Moreover, the different radii of curvature in the sagittal and in the tangential plane of the used SESAM (–5.6 m and –6.5 m, respectively) result in an increased

Optics EXPRESS

astigmatism of the output beam for a larger radius of the oscillating mode. This issue can be mitigated by optimized SESAMs with significantly larger radii of curvature as it was suggested in [33].

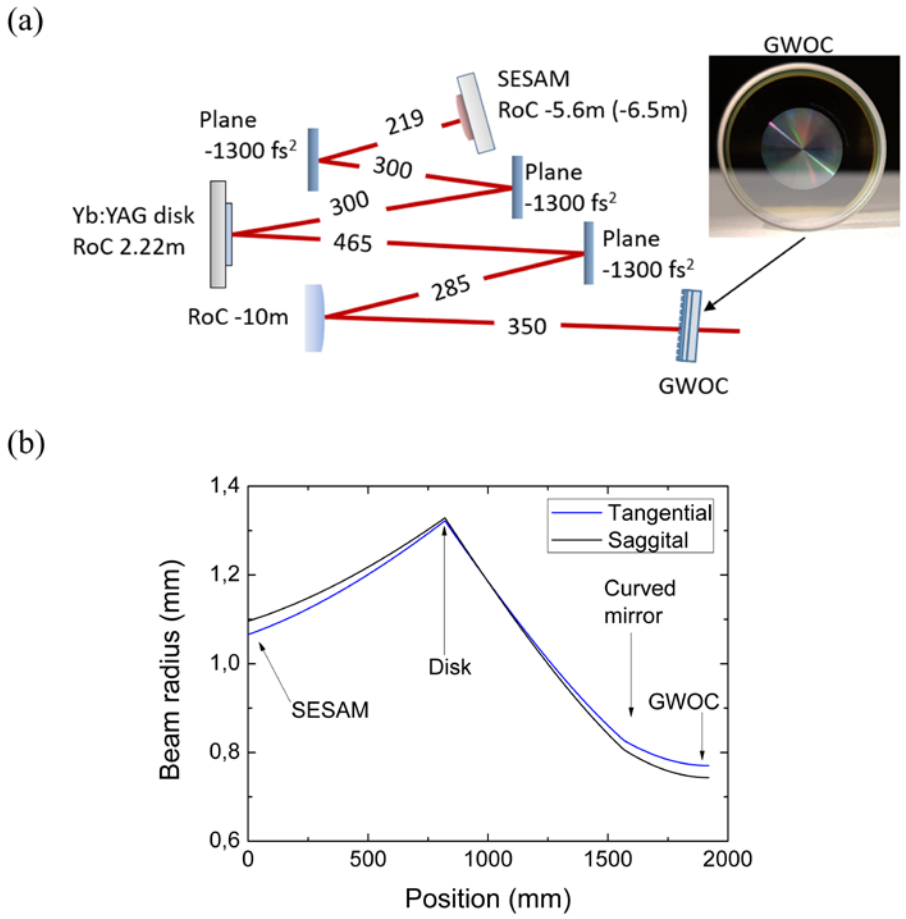

Fig. 1. (a) Sketch of the cavity consisting of the thin-disk laser crystal, the SESAM, curved mirrors with the radius of curvature (RoC, positive values correspond to concave curvatures and negative values to convex curvatures) as specified in the sketch, plane dispersive mirrors, and the GWOC (Inset: Photo of the GWOC). The distances between the cavity elements are given in mm. (b) Mode size in the cavity with position of key elements indicated by the arrows.

In order to scale the average output power as far as possible, the cavity was therefore designed to be comparatively short, with a low intra-cavity pulse energy as a result of the high repetition rate. The cavity length was reduced from around 3.5 m in [27] to 1.92 m. The resulting repetition rate of 78 MHz was almost increased by a factor of two in comparison to 42 MHz reported in our previous result [27]. One important step to reduce the cavity length was to implement a thin-disk with a smaller radius of curvature (RoC) of 2.2 m as compared to [27] where a thin-disk with an RoC of 4 m was used. Another important step for the compact cavity design was the finding that the high damage threshold of the GWOC allowed us to place this element at the beam waist (1.5 mm waist diameter) position in the cavity, see Fig. 2(b). Furthermore, as can be seen in Fig. 2(b), this cavity design avoided beam diameters smaller than 1.5 mm within the cavity which was helpful to reduce the accumulated nonlinear phase shift per roundtrip introduced by self-phase modulation. In order to balance this

Optics EXPRESS

nonlinear phase shift, three plane dispersive Gires-Turnois-interferometer (GTI) mirrors with a total group delay dispersion (GDD) of –7800 fs^2 per cavity round trip were used as folding mirrors in the cavity.

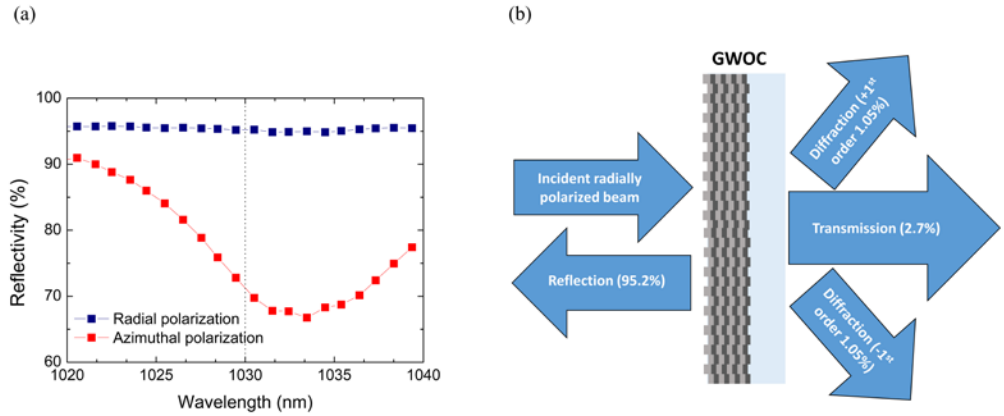

Fig. 2. (a) Spectral reflectivity of the GWOC measured with a radially and azimuthally polarized probe beam. (b) Sketch of the possible channels (reflection, transmission and diffraction) for a radially polarized beam incident on the GWOC. The out-coupled radiation is separated into the useful beam and a residual diffraction into the ± 1st diffraction order.

3. Experimental results

Figure 3 shows the measured output power and the optical efficiency that were achieved with the oscillator presented in the previous section. The laser started in cw operation at a threshold pump power of around 55.2 W and continued in this operation mode up to an output power of around 22 W. In the output power range between 22 W and 93 W the laser oscillated in Q-switched mode-locking (QML) operation. Stable self-starting continuous-wave (cw) mode-locked operation was observed at output powers exceeding 93 W. The maximum output power of 125 W was reached at a pump power of 431 W. This corresponds to an optical efficiency of 28.9%. The pump power was not increased further since a roll-over of the output power was observed which can most likely be attributed to a thermally induced drift of the resonator axis due to heating of a mirror holder by scattered laser radiation. This issue will be addressed in future developments. The noticeable step of the measured optical efficiency at a pump power of 350 W can be attributed to the manual adaption of the resonator axis for each power level. We found heated air in front of the pumped thin-disk to be the reason for the small pump power dependent misalignment of the cavity [34].

Optics EXPRESS

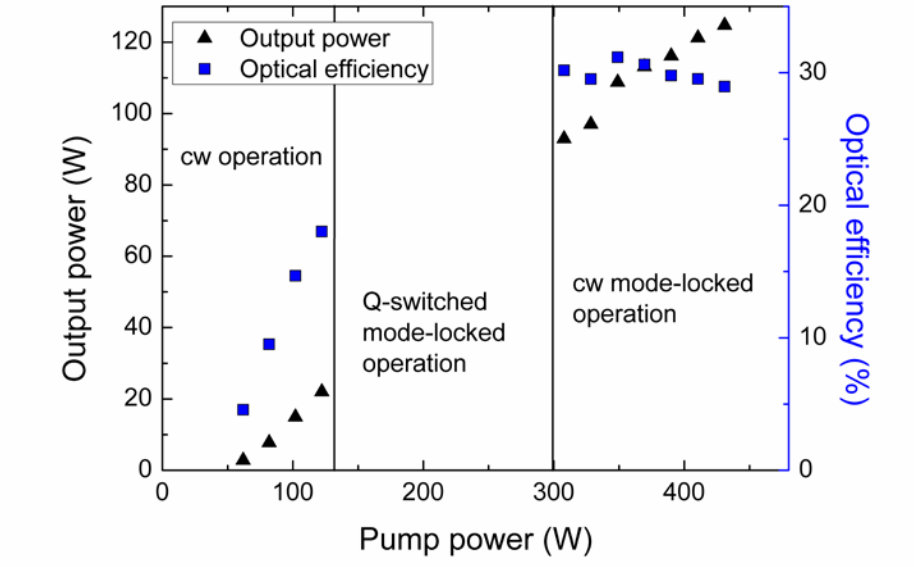

Fig. 3. Measured average output power and optical efficiency as a function of the pumping power.

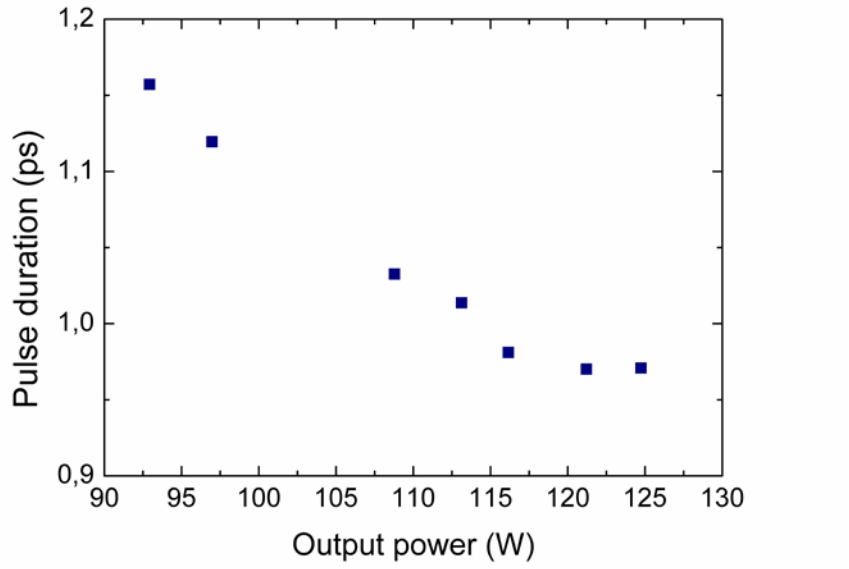

Fig. 4. Measured pulse duration over output power.

At the maximum output power of 125 W an intra-cavity average power of 4.7 kW incident on the GWOC and on the SESAM was calculated by taking into account the measured transmission of 2.7% of the GWOC. Taking into account the beam diameters in the cavity, the GWOC and the SESAM withstood average power densities of approx. 259 kW/cm^2 and approx. 124 kW/cm^2, respectively, without observation of damage. The measured pulse

Optics EXPRESS

durations ranged between 1.16 ps at an average output power of 93 W and 0.97 ps at the maximum average output power of 125 W, as can be seen in Fig. 4.

The autocorrelation trace of the pulses at the maximum power is shown in Fig. 5(a). The corresponding spectrum is shown in Fig. 5(b). It is centered at a wavelength of 1030.6 nm and exhibits a width of 1.39 nm (FWHM). This results in a time bandwidth product of 0.381 which is close to the time-bandwidth limited value of 0.315 of an ideal unchirped $sech^2$ pulse. Taking into account the repetition rate of the laser, the pulse energy and the pulse peak power at the maximum output power are 1.6 µJ and 1.45 MW, respectively. The saturation of the SESAM can be calculated by implementing the intensity distribution of the ring-shaped LG^*_{01} mode to the formula given in [35] which describes the reflectivity of the SESAM as a function of the incident pulse fluence. With this it can be shown that the saturation behavior of the SESAM is almost identical for a fundamental Gaussian mode and a LG^*_{01} mode. Taking into account the transmission of the GWOC and the pulse energy of 1.6 µJ observed at the maximum output power, the fluence on the SESAM was 1582 µJ/cm^2 which is approximately 63-times higher than the saturation fluence. It is worth mentioning that the peak intensity of the LG^*_{01} mode only amounts to 0.74 of the one of a fundamental Gaussian mode with the same beam diameter. Consequently, a roll-over of the reflectivity of the SESAM caused by two photon absorption is expected to be shifted to higher pulse energies for the LG^*_{01} mode as compared to fundamental Gaussian mode.

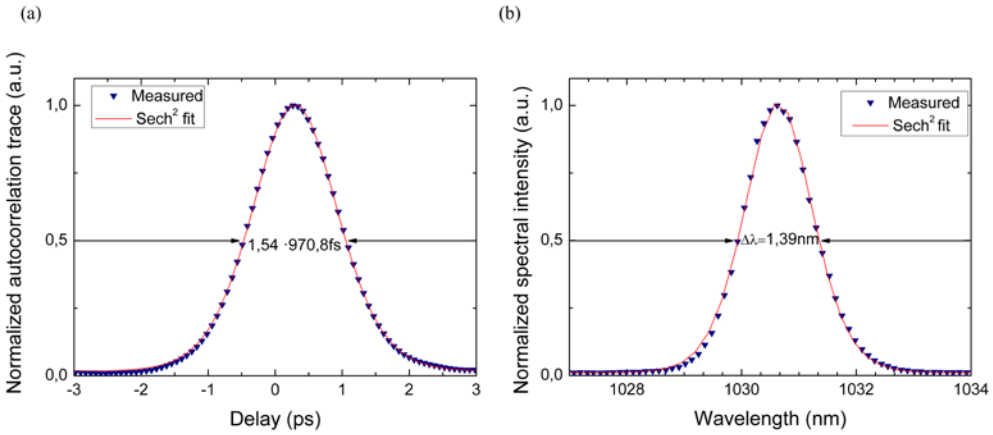

Fig. 5. (a) Second harmonic intensity autocorrelation trace and $sech^2$ fit of the pulses at maximum output power of 125 W. (b) Corresponding spectral intensity at maximum output power.

A pulse train recorded with a photodiode with rise time of about 200 ps on an oscilloscope with a sampling rate of 5 GS/s and a bandwidth of 1 GHz is shown in Fig. 6. The pulses are separated by the cavity roundtrip time of 12.8 ns. Thus, satellite pulses with a temporal distance of more than ~600 ps can be excluded from this measurement.

Optics EXPRESS

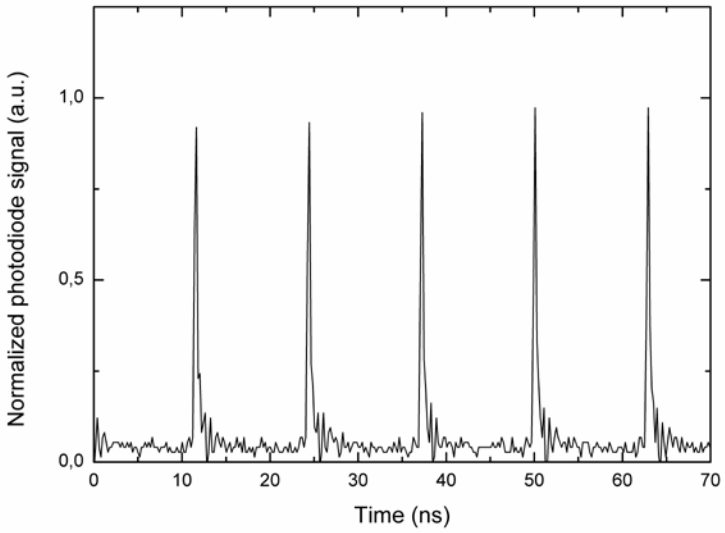

Fig. 6. Pulse train measured with a fast photodiode on an oscilloscope.

The radio frequency spectrum measured at the maximum output power is shown in Fig. 7. The absence of side peaks further confirms the stable mode-locked operation. Despite the low signal-to-noise ratio of this measurement no relaxation oscillations were observed in the RF-spectra at pump powers above 300 W, indicating fundamental mode-locking. Side peaks were clearly visible on the RF analyzer only when the oscillator was operated in the QML regime at pump powers from around 130 W to 300 W (see Fig. 3). Using a more suitable photodiode will enable improved measurements in future works. An additional long range autocorrelation measurement with a range of ± 75 ps to each side of the pulse confirmed single-pulse mode-locked operation in this temporal window. Nevertheless, there is a temporal window from 75 ps to ~600 ps where satellite pulses cannot be excluded with certainty. However, the decreasing pulse duration for higher output powers (see Fig. 4) indicate single pulse operation over the complete range of output power.

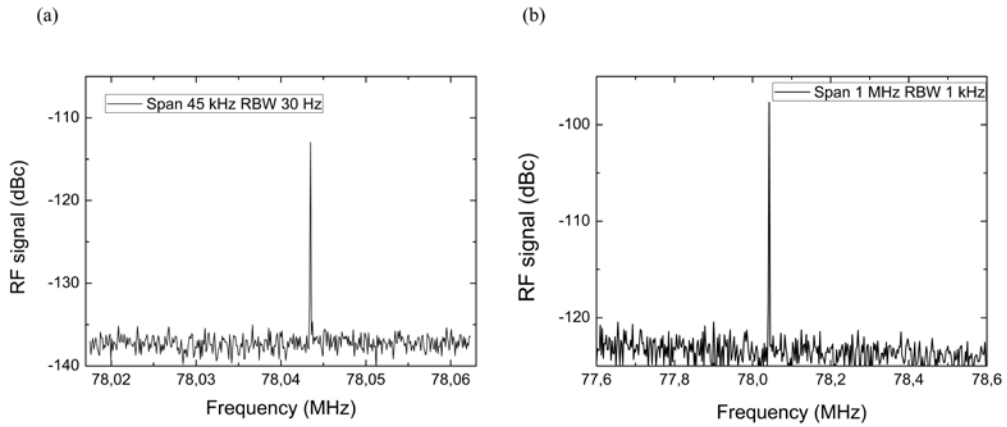

Fig. 7. (a) Radio frequency signal measured with a span of 45 kHz and a Resolution Bandwidth (RBW) of 30 Hz. (b) Radio frequency signal measured with a span of 1 MHz and a RBW of 1 kHz.

Optics EXPRESS

The far-field beam profile recorded at the maximum output power is shown by the upper left image in Fig. 8. The intensity distribution is not perfectly symmetric, which is a result of a shift of the oscillating mode on the GWOC, caused by the abovementioned thermal drift of the resonator axis. Nevertheless, the M^2-values of 2.15 and 2.16 in the tangential and sagittal plane, respectively, measured at the maximum output power are close to the theoretical value of 2.0 expected for the LG^*_{01} mode. The polarization purity was qualitatively analyzed by a rotating polarization analyzer in the beam path as shown by the images with the white arrows in Fig. 8. The white arrows indicate the polarization of the radiation transmitted through the polarizer. The well separated lobes indicate a high radial polarization purity. This was confirmed by a measurement with a 2D Stokes-polarimeter [36] which yielded a degree of radial polarization of 97.3 ± 1%.

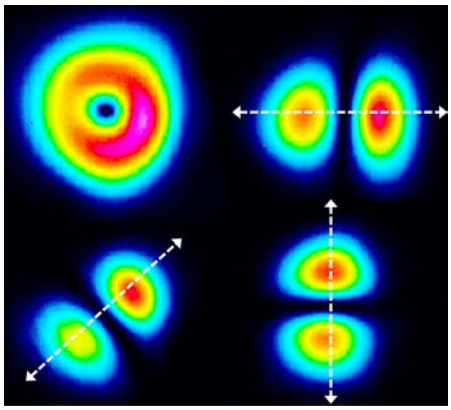

Fig. 8. Far-field intensity distribution and intensity distribution transmitted through a rotatable polarization analyzer. The white arrows indicate the direction of the polarization.

4. Conclusion

In summary, we have demonstrated a radially polarized Yb:YAG passively mode-locked thin-disk laser oscillator providing an average output power exceeding the 100 W power level. An average output power of 125 W was achieved at a pump power of 431 W. To the best of our knowledge this is the highest average output power of a radially polarized mode-locked laser oscillator reported to date and corresponds to an improvement of almost one order of magnitude as compared to previous reports. With a pulse repetition rate of 78 MHz and the measured pulse duration of 0.97 ps this corresponds to a pulse energy of 1.6 µJ and a peak power of 1.45 MW, respectively. Thanks to the achieved power level this oscillator is a promising seed for further power scaling into the kW power range by means of thin-disk multipass amplifiers and significantly reduced the overall complexity of the system as compared to the previous state of the art.

Funding

European Union Seventh Framework Programme (FP7/2007-2013, 619237); IGF-Projekt 18728 N.

Acknowledgment

We would like to thank the ITO (Institut für Technische Optik) for the production of the GWOC.